DOI: 10.17344/acsi.2021.6819 *Acta Chim. Slov.* **2022,** *69,* 30–38

Scientific paper

Glucose-Decorated Silica-Molybdate Complex: A Novel Catalyst for Facile Synthesis of Pyrano[2,3-d]-Pyrimidine Derivatives

Arezoo Pourkazemi, Negin Asaadi, Mahnaz Farahi,* Ali Zarnegaryan and Bahador Karami

Department of Chemistry, Yasouj University, P. O. Box 353, Yasouj 75918-74831, Iran

** Corresponding author: E-mail: farahimb@yu.ac.ir*

Received: 03-13-2021

Abstract

This article describes the preparation and identification of SiO_2@Glu/Si(OEt)$_2$(CH$_2$)$_3$N = Mo[Mo_5O_{18}] as a new bifunctional acid-base catalyst (both acidic and basic Lewis sites). Aminopropyltriethoxysilane was first reacted with hexamolybdate anions and then treated with glucose to prepare Glu/Si(OEt)$_2$(CH$_2$)$_3$N = Mo[Mo_5O_{18}]. Nano-silica was then modified by the prepared glucose/molybdate complex to obtain SiO_2@Glu/Si(OEt)$_2$(CH$_2$)$_3$N = Mo[Mo_5O_{18}]. The developed catalyst was characterized by FT-IR, EDX, XRD, FE-SEM and TGA analyzes. Its catalytic efficiency was investigated for the preparation of pyrano[2,3-*d*]pyrimidine derivatives by the reaction between various aldehydes, malononitrile and barbituric acid. The desired products were prepared in the presence of 0.004 g of the prepared catalyst in high to excellent yields.

Keywords: Silica nanoparticle; glucose; hexamolybdate anions; pyrano[2,3-*d*]pyrimidine; nanocatalyst

1. Introduction

Catalysis includes the variants of homogeneous, heterogeneous, and biological catalysis. Homogeneous catalysts offer many distinct advantages over their heterogeneous counterparts. For example, due to the high solubility of homogeneous catalysts, all catalytic sites are accessible. In addition, they often exhibit high chemoselectivity, regioselectivity, and/or enantioselectivity in organic transformations.[1] Despite these advantages, most homogeneous catalysts have not been used commercially because they have one major disadvantage compared to heterogeneous catalysts: They are difficult to separate from the reaction mixture and solvent. The usual separation method requires high temperatures, while most homogeneous catalysts are thermally sensitive and usually decompose below 150 °C.[2] Attempts have been made to solve the problem by immobilizing the catalysts on various supports such as carbon, silica, metal oxide, polymers, and nanocomposites.[1] Over the past century, the development of recoverable supported catalysts with high efficiency has been the subject of much research. Immobilized catalysts have significant advantages such as ease of handling, low solubility, possibility of recovery, and low toxicity.[3-8] In heterogeneous supported catalysis, the catalytic ability of materials usually depends on their microscopic structure, which directly affects the activity, selectivity, and thermal or chemical stability of the catalyst.[9] Nanomaterials are widely used as solid support materials for the preparation of many heterogeneous catalytic systems to solve various economic and environmental problems.[10] Nano-silica is widely used due to its unique properties, such as controllable particle size and non-toxicity. Nano-SiO_2 has a high surface-to-volume ratio and a porous structure that enables high chemical reactivity.[11] In addition, nano-silica has been used in various fields such as biomedicine, fillers, catalysis, and drug delivery systems. The size and uniformity of nano-silica particles have the greatest influence on their quality; therefore, SiO_2 nanoparticles with narrow and monodisperse size distribution are increasingly in demand.[12–14] Compared with the well-known methods for preparing nano-SiO_2, the Stöber method is considered to be the most effective method for preparing monodisperse silica spheres. This method provides a flexible chemical route to fabricate materials that are highly pure, chemically reactive, and well dispersed.[15]

The great attention given to nanoparticles is due to their exceptional properties: easy availability, chemical in-

ertness, high surface-to-volume ratio, high activity and selectivity, thermal stability, and low toxicity. Moreover, nanoscale systems significantly increase the contact between reactants and catalyst. They open new perspectives for mild catalysis of important reactions with lower environmental impact. Nanoparticles differ from their solid counterparts and exhibit special properties. Due to the above advantages, they have been developed as suitable replacements for conventional heterogeneous catalysts.[16]

Recently, inorganic-organic hybrid materials have been widely used as catalysts for organic reactions because they are well suited for various processes of environmentally friendly chemical transformations.[17] Several interesting new materials with novel properties are currently emerging in this rapidly growing field. They combine the typical advantages of organic components, such as flexibility, low density, toughness, and malleability, with the advantages of typical inorganic materials, such as hardness, chemical resistance, strength, and optical properties.[18] The properties of these materials are not just the sum of the individual contributions of the two phases, but the role of the internal interfaces could also be important. Organic-inorganic graft materials have emerged as surrogate materials for the development of unique products and have become a new area of academic research.

When the idea of a monomolecular bifunctional catalyst for helpful catalysis was first introduced in 2003, both homogeneous and heterogeneous catalysts with molecular design and their use in organic reactions became the focus of interest.[19] In this context, polyoxometalates (POMs) are an important class of nanoscale polynuclear clusters with significant physical and chemical properties based on transition metals in their highest oxidation states and oxygen bridges.[20] Polyoxometalate clusters, known for their enormous size and interesting properties for medicine and nonlinear optics, are a prominent class of linkers for the preparation of interpenetrating networks. The direct application of POM clusters as linkers promises an attractive route to the development of new entangled network structures. The main properties of polyoxometallates and the variation in their structures give them great potential for applications in various fields of chemical processing.[21] Despite the above advantages, the solubility and non-recoverability of POMs in various media limit their applications in some processes. Immobilization of these clusters on solid supports such as silica and magnetic nanoparticles could be an important way to overcome this problem. Hexamolybdates are a group of POMs used in various inorganic and organic reactions due to their thermal stability and radiation resistance. Lindqvist hexamolybdate cluster, $[Mo_6O_{19}]^{2-}$, as a unique class of metal oxide clusters, is an ideal building block for the construction of organic–inorganic hybrid assemblies.[22,23]

Carbon-based materials have attracted much attention from researchers because they are environmentally friendly, cheap, and nontoxic. Numerous studies have been conducted on these materials as catalyst supports, such as carbon nanotubes, carbon-polymer composites, mesoporous carbons, graphitized carbons, graphitized nitride carbons, carbides, and carbon aero-gels. In this context, cellulose has been used as a catalyst support due to its uniform shape, stability in aqueous solution, good mechanical strength, high specific surface area, biocompatibility and biodegradability. The development of cellulose-based composites with metal oxides such as silicon dioxide, titanium dioxide, zinc oxide, and iron oxides is of great interest for various high-technology applications.[24-26] Due to its polyhydroxy structure, glucose has been used as the main green monosaccharide catalyst and showed excellent catalytic activity in chemical reactions such as epoxidation and enantioselective Michael addition. It has also played the role of a green medium for carrying out reactions. Recently, Fe_3O_4 nanoparticles coated with glucose were prepared and used as a heterogeneous catalyst for the synthesis of pyrazole derivatives.[27]

Nowadays, several chemists have paid great attention to the development of new approaches to the production of nitrogen-containing heterocycles, which play an important role in our lives. They are components of many natural products, fine chemicals, and biologically active drugs that are of great importance in improving the quality of life.[28] Pyrano[2,3-*d*]pyrimidine derivatives represent a "privileged" structural motif that is widely used in naturally occurring compounds with a variety of important biological properties. Recently, a number of synthetic pyrano[2,3-*d*]pyrimidines have been investigated for their potent anticancer, antibacterial, antifungal, and antirheumatic properties.[29] They also exhibit anti-inflammatory,[30] anti-HIV,[31] cytotoxic,[32] antimicrobial,[33] antimalarial, and antihyperglycemic properties.[34] It is worth noting that many drug molecules bearing the pyrano-pyrimidine moiety are used in the treatment of various diseases such as bronchitis, as hepatoprotective agents, and as cardiotonic agents.[33]

With increasing public concern about environmental degradation and future resources, it is critical for chemists to develop new approaches that are less hazardous to human health and the environment. Therefore, in conjunction with our previous research on new heterogeneous catalysts,[35-41] we decided to introduce SiO_2@Glu/$Si(OEt)_2(CH_2)_3N = Mo[Mo_5O_{18}]$ nanocatalysts, whose catalytic activity was investigated in the one-pot synthesis of pyrano[2,3-*d*]pyrimidines.

2. Results and Discussion

The desired catalyst was synthesized in a simple manner as shown in Scheme 1. To prepare SiO_2@Glu/$Si(OEt)_2(CH_2)_3NH_2$ grafted $[Mo_6O_{19}]^{2-}$ composite (**3**), 3-aminopropyltriethoxysilane was reacted with tetrabutylammonium hexamolybdate followed by glucose to give

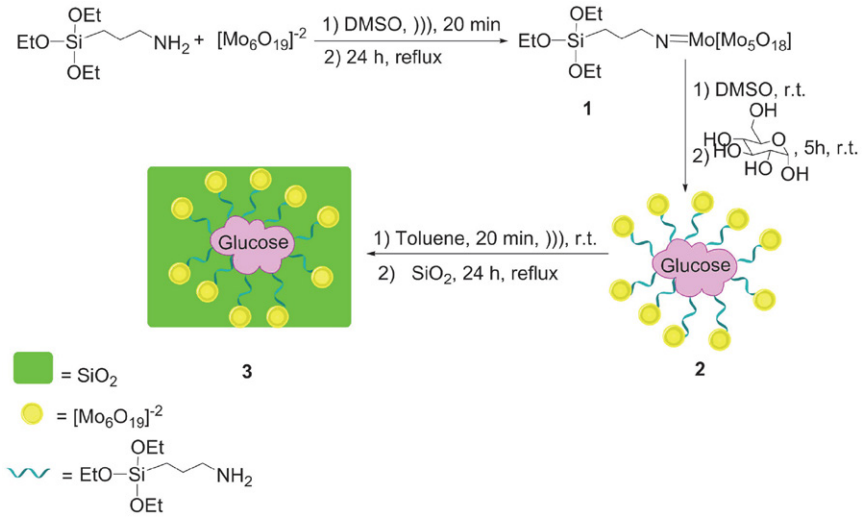

Scheme 1. Schematic representation of the synthesis of SiO_2@Glu/$Si(OEt)_2(CH_2)_3N$ = $Mo[Mo_5O_{18}]$ (**3**).

Glu/$Si(OEt)_2(CH_2)_3N$ = $Mo[Mo_5O_{18}]$ (**2**). SiO_2 nanoparticles were also synthesized by the Stöber method.[15] Finally, the OH groups on the silica surface can be grafted with Glu/$Si(OEt)_2(CH_2)_3N$ = $Mo[Mo_5O_{18}]$ to obtain the desired nanocatalyst **3**. The chemical and structural properties of the catalyst were investigated by FT-IR, EDX, XRD, FE-SEM and TGA analyzes.

The identification and determination of the organic functional groups were performed by FT-IR spectroscopy. Figure 1 shows the infrared spectra of glucose, SiO_2, SiO_2@Glu/$Si(OEt)_2(CH_2)_3N$ = $Mo[Mo_5O_{18}]$ and $[n\text{-}Bu_4N]_2[Mo_6O_{19}]$. In Figure 1a, the peaks at 3662 and 3385 cm^{-1} are assigned to the OH groups. Also, the peaks at 2939 and 1458 cm^{-1} are related to the stretching of CH and the symmetric bending stretching of CH_2, respectively. The bands at 1160 cm^{-1} (antisymmetric C-O-C stretching), 1116 cm^{-1}, and 1052 cm^{-1} (skeletal vibrations with C-O stretching) can be assigned.[18] Figure 1b shows the bands at 1080, 948, and 797 cm^{-1} that are due to Si-O stretching, Si-OH stretching, and symmetric Si-O-Si stretching, respectively.[15] In Figure 1c, the absorption peaks at 2934 and 2840 cm^{-1} correspond to the C-H vibrations of the alkyl chains.[35] Moreover, the bands at 953, 804, and 798 cm^{-1} are attributed to N = Mo, Mo-O, and Mo-O-Mo, respectively, confirming the presence of $[Mo_6O_{18}]^{-2}$ ions in the structure of the synthesized nanocatalyst.[22]

The XRD patterns of SiO_2@Glu/$Si(OEt)_2(CH_2)_3N$ = $Mo[Mo_5O_{18}]$ and SiO_2 are shown in Figure 2, which was used to study the crystallographic features of the prepared catalyst. It can be seen that the reflection peaks are in the 2θ range of 0–70°. In Figure 2a, the broad peak in the 2θ 20°–32° range is consistent with an amorphous silica phase.[36] The presence of sharp peaks proves the special status of the nanocatalyst structure. In Figure 2b, the XRD pattern shows that the amorphous structure of SiO_2 particles was preserved. The confirming peak indicating the

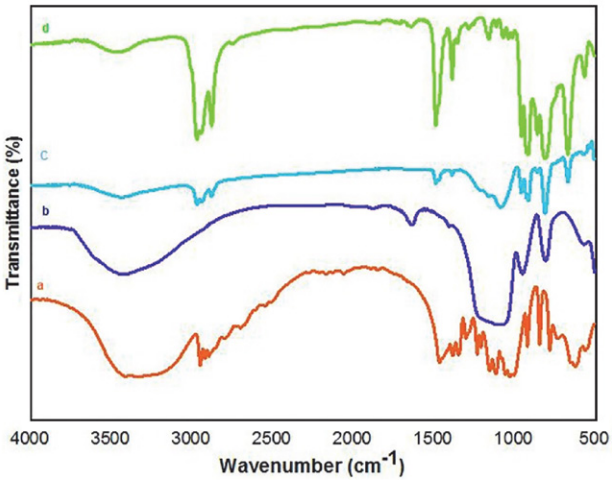

Figure 1. FT-IR Spectra of a) glucose, b) SiO_2, c) SiO_2@Glu/$Si(OEt)_2(CH_2)_3N$ = $Mo[Mo_5O_{18}]$ and d) $[n\text{-}Bu_4N]_2[Mo_6O_{19}]$.

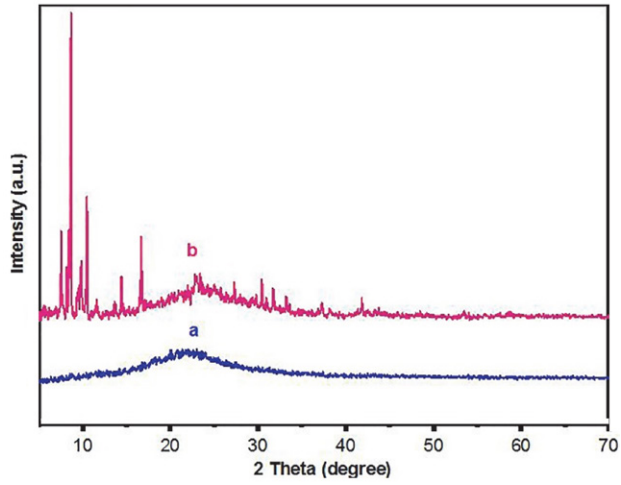

Figure 2. The XRD pattern of a) SiO_2 and b) SiO_2@Glu/$Si(OEt)_2(CH_2)_3N$ = $Mo[Mo_5O_{18}]$ nanocatalyst.

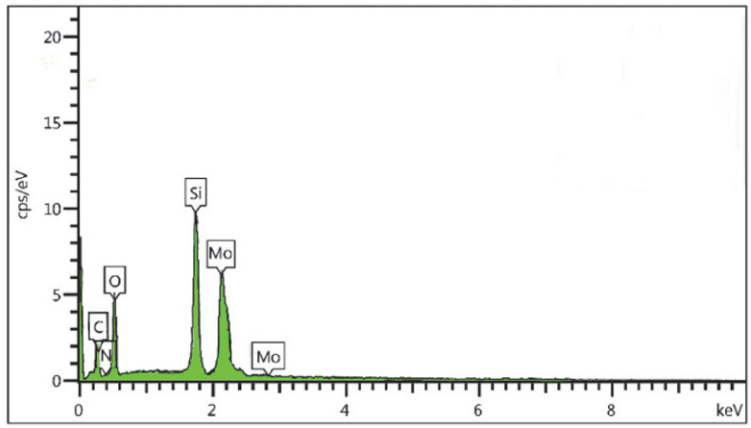

Figure 3. EDS analysis of SiO_2@Glu/Si(OEt)$_2$(CH$_2$)$_3$N = Mo[Mo_5O_{18}].

presence of the molybdate group appeared in the range of 2θ = 20°–30°, which can be attributed to the amorphous molybdate on the composite.[35,39]

Energy-dispersive X-ray spectroscopy (EDS) was selected to provide the necessary information on elemental structure of the catalyst. According to the Fig. 3, the EDS pattern clearly indicated the existence expected the elemental composition of C, N, O, Si, and Mo in the nanocatalyst structure.

The surface morphology and particle size distribution of the prepared nanocatalyst were observed using FE-SEM, and the corresponding image is shown in Figure 4. The results show that the particles are uniformly and regularly spherical with an average diameter of 22–42 nm.

The results of the thermal stability of nanocatalyst **3** by thermogravimetric analysis (TG) from 0 to 900 °C are shown in Figure 5. The results show that the first weight loss at a temperature of 120 °C (about 12%) is related to the removal of H_2O and other organic solvents left behind in the extraction process. The second weight loss at 220–320 °C (about 5%) is due to the removal of organic components located on the surface of the catalyst. The largest weight loss in a temperature range of 500–550 °C (about 12.5%) is related to the removal of propylamine groups attached to the catalyst framework.[22]

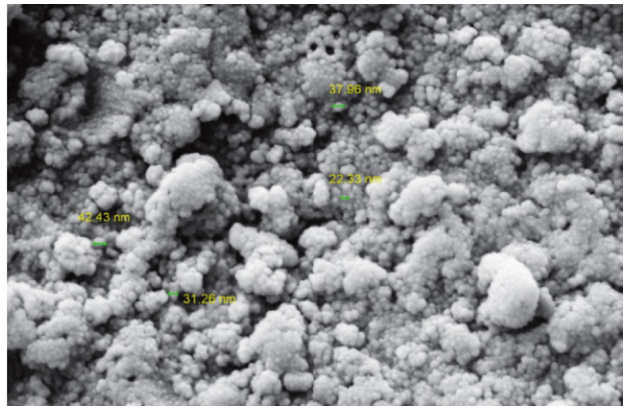

Figure 4. FE-SEM analysis of SiO_2@Glu/Si(OEt)$_2$(CH$_2$)$_3$N = Mo[Mo_5O_{18}].

After characterization to study the catalytic activity and efficiency of the newly developed catalyst, it was used as a catalyst for the synthesis of pyrano[2,3-*d*]pyrimidines **7** via the three-component reaction of arylaldehydes **4**,

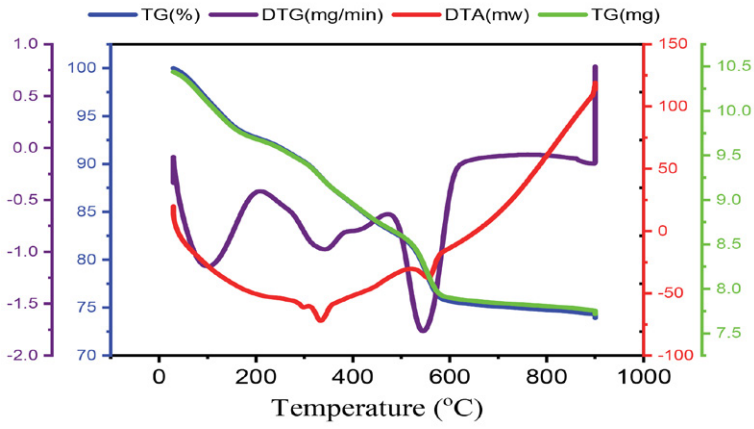

Figure 5. TG analysis of SiO_2@Glu/Si(OEt)$_2$(CH$_2$)$_3$N = Mo[Mo_5O_{18}].

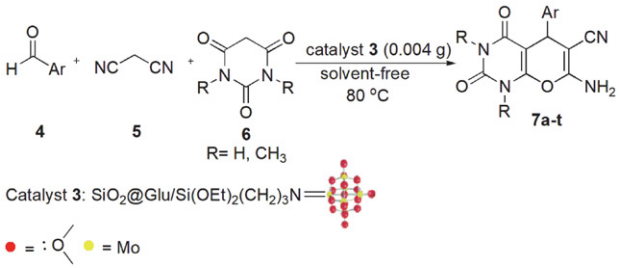

Scheme 1. Preparation of pyrano[2,3-*d*]pyrimidines **7** in the presence of SiO_2@Glu/Si$(OEt)_2(CH_2)_3N$ = Mo$[Mo_5O_{18}]$ nanocatalyst.

malononitrile **5**, and barbituric acid **6** under solvent-free conditions (Scheme 2).

To find the optimum reaction conditions, a three-component reaction between benzaldehyde, malononitrile, and 1,3-dimethylbarbituric acid was selected as a model reaction, and the effect of various parameters such as temperature, catalyst loading, and solvent was evaluated. The reaction did not proceed well in the absence of the catalyst after a long reaction time. The model reaction was carried out at 25, 60, 80 and 100 °C in the presence of 0.002 g catalyst **3**. The study showed that the reaction was affected by temperature, and the best result was observed at 80 °C. Next, the effect of the amount of catalyst was studied. It was found that the yield increased when the amount of catalyst was increased from 0.002 g to 0.004 g, and higher amount of catalyst did not have a good effect on the reaction process. Moreover, the model reaction was carried out with 0.004 g SiO_2@Glu/Si$(OEt)_2(CH_2)_3N$ = Mo$[Mo_5O_{18}]$

Table 1. Screening of various parameters in the synthesis of **7a** catalyzed by nanocatalyst **3**.[a]

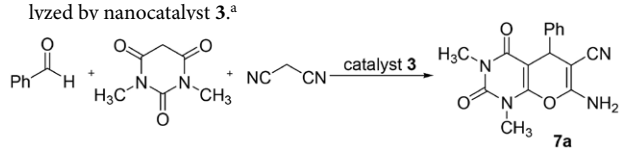

Entry	Catalyst loading (g)	Solvent	Temp. (°C)	Yieldb (%)
1	0.002	–	25	20
2	0.002	–	60	45
3	0.002	–	80	60
4	0.002	–	100	50
5	0.004	–	80	90
6	0.006	–	80	85
7	0.008	–	80	80
8	0.004	MeOH	Reflux	60
9	0.004	EtOH	Reflux	70
10	0.004	CH3CN	Reflux	75
11	0.004	Toluene	Reflux	65

[a] Reaction conditions: benzaldehyde (1 mmol), malononitrile (1 mmol), 1,3–dimethylbarbituric acid (1 mmol), time: 20 min. [b] Isolated yields.

Table 2. Preparation of various pyrano[2,3-*d*]-pyrimidines by nanocatalyst **3**.

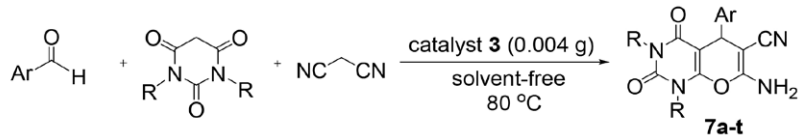

Entry	R	Aldehyde	Tim (min)	Yield[a] (%)	Mp (Lit) (°C)
7a	H	C6H5CHO	30	90	212–214 (212–213)[42]
7b	H	2,4-Cl C6H3CHO	15	93	242–244 (242–243)[42]
7c	H	3-NO2 C6H4CHO	20	95	260–262 (262–263)[43]
7d	H	4-NO2 C6H4CHO	20	93	237–239 (237–238)[43]
7e	H	3-Br C6H4CHO	25	95	280–282 (279–280)[43]
7f	H	4-Br C6H4CHO	20	90	228–230 (227–229)[43]
7g	H	4-OCH3 C6H4CHO	25	95	280–282 (281–282)[43]
7h	H	4-Cl C6H4 CHO	15	90	238–240 (239–240)[44]
7i	CH3	C6H5CHO	20	95	228–230 (228–229)[44]
7j	CH3	2-Cl C6H4 CHO	15	89	248–250 (250–251)[44]
7k	CH3	4-OCH3 C6H4CHO	30	95	224–225 (225–227)[44]
7l	CH3	4-Cl C6H4CHO	10	95	238–240 (239–241)[44]
7m	CH3	3-NO2 C6H4CHO	20	93	212–214 (212–213)[44]
7n	CH3	4-NO2 C6H4CHO	20	95	230–232 (231–232)[44]
7o	CH3	3-Br C6H4CHO	15	93	218–220 (218–219)[44]
7p	CH3	4-CH3 C6H4CHO	20	90	230–232 (229–230)[44]
7q	CH3	2,4-Cl2 C6H3CHO	10	95	211–213 (211–212)[30]
7r	CH3	1-Naphthaldehyde	40	93	360 (360–361)[44]
7s	CH3	Biphenyl-4-carboxaldehyde	30	95	275–277[b]
7t	CH3	Terephthalaldehyde	20	95	240–242[b]

[a] Isolated yields. [b] Novel product.

in some solvents such as methanol, ethanol, acetonitrile and toluene. As can be seen, considerable acceleration is observed especially for reactions carried out under solvent-free conditions. According to these results, the use of SiO_2@Glu/$Si(OEt)_2(CH_2)_3N$ = $Mo[Mo_5O_{18}]$ (0.004 g) as catalyst under solvent-free conditions at 80 °C would be the best choice (Table 1).

After optimization of the reaction conditions, the reaction of various aromatic aldehydes, malononitrile and barbituric acid derivatives was studied in the presence of nanocatalyst **3** under optimal conditions, which showed the successful formation of the corresponding pyrano[2,3-*d*]-pyrimidines (Table 2). Both aldehydes with electron-donating groups and aldehydes with electron-attracting groups were prepared in good to excellent yields.

The proposed mechanism for the formation of pyrano[2,3-*d*]pyrimidines **7** is shown in Scheme 3. According to the proposed mechanism, adduct **8** is first obtained by the condensation of aromatic aldehydes and malononitrile in the presence of the catalyst. Then, Michael addition of barbituric acid to this intermediate **9** is formed. The intramolecular cyclization of **9** gives the adduct **10**, which rearranges to give the pyrano[2,3-*d*]pyrimidinones **7**.

The main advantages of the presented protocol over existing methods become clear when our results are compared with those of some recent methods reported in articles (see Table 3).

To study the leaching of $[Mo_6O_{19}]^{2-}$ from SiO_2@Glu/$Si(OEt)_2(CH_2)_3N$ = $Mo[Mo_5O_{18}]$, we performed an in situ filtration technique. When the model reaction reached 50%, warm EtOAc (5 ml) was added, and catalyst isolation was performed by simple filtration. After removal of the solvent, the process was continued with the catalyst-free residue under the previously optimized conditions. As expected, the reaction stopped, confirming that no leaching of the supported catalytic centers occurred under the optimized conditions. The reusability of SiO_2@Glu/$Si(OEt)_2(CH_2)_3N$ = $Mo[Mo_5O_{18}]$ was also investigated in the model reaction. After completion of the reaction, EtOAc (5 mL) was added to the mixture, the catalyst was filtered, washed with EtOH (10 mL) and deionized water (10 mL), and then dried at 100 °C. The recovered catalyst was used ten times in the model reaction, and the yield was negligible (Figure 6). These experiments indicate high stability and durability of this nanocatalyst under the applied conditions. To test the stability of the catalyst structure, the recycled nanocatalyst was examined using FT-IR spectra. The FT-IR spectra of the freshly prepared catalyst and the recycled catalyst are shown in Figure 7 and confirm the chemical stability of catalyst **3**.

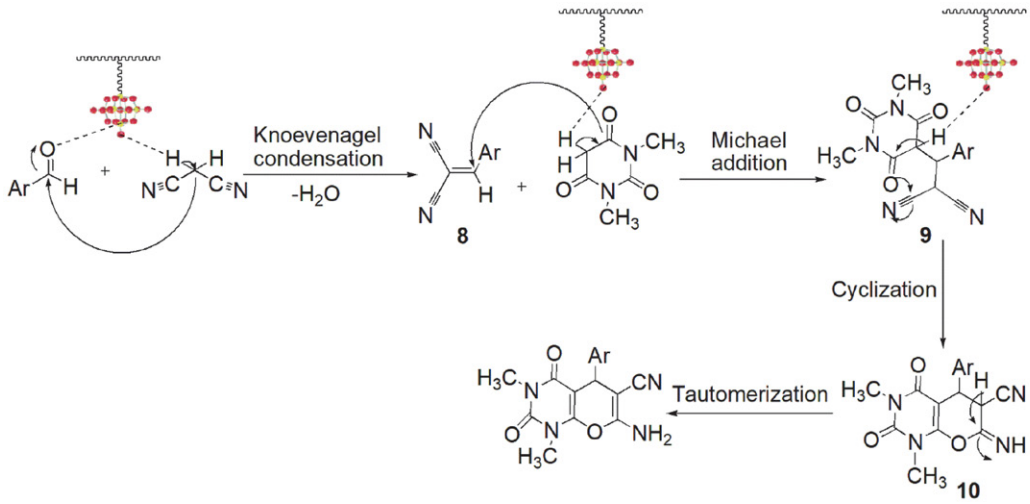

Scheme 3. The proposed mechanism for the synthesis of pyrano[2,3-*d*]pyrimidinones catalyzed by nanocatalyst **3**.

Table 3. Comparison of results for the synthesis of **7I** with other catalysts.

Entry	Catalyst	Catalyst loading	Condition	Time (min)	Yield[a] (%)[a]
1	Catalyst **3**	0.004 g	solvent-free, 80 °C	10	95[b]
2	Et_3N	20 mol %	EtOH, 50 °C	25	87[28]
3	Urea	10 mol %	EtOH:H_2O, r.t.	840	86[29]
4	Zn [(L) proline]$_2$	17 mol %	EtOH, Reflux	50	90[45]
5	{Fe_3O_4@SiO_2@$(CH_2)_3$-Urea-SO_3H/HCl} MNP	0.01 g	solvent-free, 60 °C	30	97[44]
6	Nano-basic silica	25 mol %	solvent-free	54	89[46]

[a] Isolated yields. [b] This study.

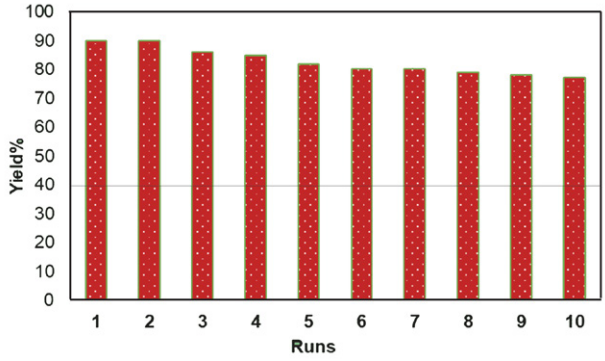

Figure 6. Reuse of SiO_2@Glu/Si(OEt)$_2$(CH$_2$)$_3$N = Mo[Mo_5O_{18}] nanocatalyst.

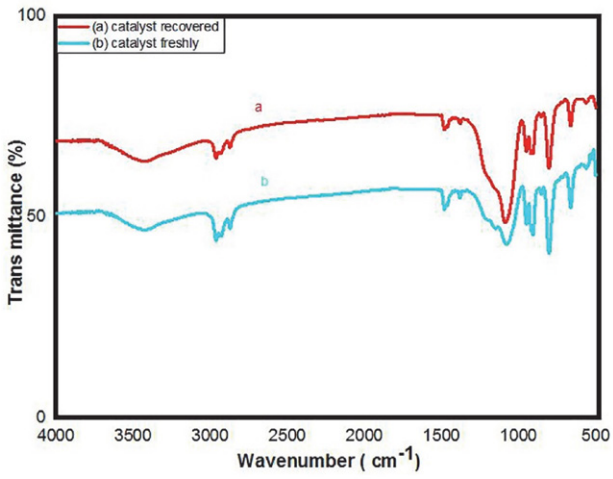

Figure 7. FT-IR spectra for comparison of fresh catalyst and recovered catalyst.

3. Experimental

All chemical materials were purchased from Merck and Aldrich. The reaction progress and purity of the compounds were monitored by TLC on silica gel SIL G/UV254 plates. Melting points were checked using a KSB1N electrothermal device and are correct. The IR spectra of all synthesized compounds were recorded in the KBr matrix using a spectrometer model JASCO FT-IR /680 plus. ^{1}H NMR spectra were recorded in DMSO-d_6 as solvent using a Bruker Avance Ultra Shield 400 MHz spectrometer, and ^{13}C NMR spectra were registered at 100 MHz. A scanning electron microscope (FE-SEM) was used to measure the size of the particles and the shape of the catalyst. X-ray diffraction (XRD) patterns were recorded with a Philips X Pert Pro X diffractometer using Ni filtered Cu-Ka radiation. Energy dispersion spectroscopy (EDS) was recorded using a TESCAN Vega instrument.

Preparation of the Glu/Si(OEt)$_2$(CH$_2$)$_3$N = Mo[Mo_5O_{18}]

First, the tetrabutylammonium hexamolybdate ([n-Bu4N]2 [Mo6O19]) was prepared according to the described procedure.[20] The tetrabutylammonium hexamolybdate (0.4 g) and DMSO (20 ml) were placed in a round bottom flask (50 ml) and dispersed for 20 minutes. Then 3-aminopropyltriethoxysilane (2.5 ml) was added dropwise to the mixture and stirred under reflux conditions for 24 hours under argon atmosphere. Dissolved glucose (0.26 g) in dry DMSO (5 mL) and H_2SO_4 (98%, 0.33 mL) were then added. The mixture was stirred at room temperature for 5 hours. Finally, the obtained product (compound **2**) was washed with ethanol, distilled and dried at 80 °C.

Protocol for the synthesis of nano-SiO_2

Tetraethyl orthosilicate (TEOS) (6.2 ml) was added to ethanol (100 ml) and ammonium hydroxide (6.5 ml), and the mixture was stirred at room temperature for 15 hours. The mixture was then filtered by centrifugation (4000 rpm, 30 min), and the resulting white powder was washed three times with ethanol and dried for 12 h at 60 °C.[15]

Preparation of the SiO_2@Glu/Si(OEt)$_2$(CH$_2$)$_3$N = Mo[Mo_5O_{18}]

To immobilize Glu/Si(OEt)$_2$(CH$_2$)$_3$N = Mo[Mo_5O_{18}] on the surface of SiO_2, the prepared SiO_2 nanoparticles (1.0 g) were dispersed in dry toluene (30 mL) by ultrasonication for 20 min. Compound **2** (0.5 g) was then added and the mixture was refluxed under argon atmosphere for 24 hours. Then the prepared SiO_2@Glu/Si(OEt)$_2$(CH$_2$)$_3$N = Mo[Mo_5O_{18}] was filtered and washed several times with ethanol and then with water. Finally, the brown powder was dried in vacuo at 80 °C for 24 hours.

General procedure for the synthesis of pyrano[2,3-*d*]-pyrimidines derivatives 7

SiO_2@Glu/Si(OEt)$_2$(CH$_2$)$_3$N = Mo[Mo_5O_{18}] (0.004 g) was added to the mixture of arylaldehyde (1 mmol), malononitrile (1 mmol), and barbituric acid (1 mmol) at 80 °C under solvent-free conditions. The progress of the reaction was monitored by TLC. After completion of the reaction, ethyl acetate was added and the catalyst was separated by filtration. For further purification of the product, the obtained powder was recrystallized from EtOH.

Spectral data

*7-Amino-5-(2,4-dichlorophenyl)-1,3-dimethyl-2,4-dioxo-1,3,4,5-tetrahydro-2H-pyrano[2,3-d]pyrimidine-6-carbonitrile (**7q**).* White solid; mp: 211–213 °C; IR (KBr) (ν_{max}, cm^{-1}) 3394, 3313, 3212, 3081, 2962, 2194, 1708, 1689, 1643, 1494, 1384, 1230, 1184, 1099, 1049, 844, 582, 755. ^{1}H NMR (400 MHz, DMSO-d_6) δ 3.09 (s, 3H), 3.39 (s, 3H), 4.88 (s, 1H), 6.93-7.55 (m, 5H) ppm. ^{13}C NMR (100 MHz, DMSO-d_6) δ 28.09, 29.63, 33.70, 57.19, 88.07, 118.86, 128.12, 129.01, 132.11, 132.44, 133.67, 140.85, 150.44, 151.05, 158.22, 160.78 ppm.

*5-([1,1'-Biphenyl]-4-yl)-7-amino-1,3-dimethyl-2,4-dioxo-1,3,4,5-tetrahydro-2H-pyrano[2,3-d]pyrimidine-6-carbonitrile (**7s**).* White solid; mp: 275–277 °C; IR (KBr) (ν_{max}, cm^{-1}) 3432, 3300, 3177, 3074, 2984, 2190, 1736, 1684, 1634, 1486, 1386, 1227, 1186, 1040, 1007, 850, 744, 751, 698, 571, 550. ^{1}H NMR (400 MHz, DMSO-d_6) δ 2.11 (s, 3H), 2.54 (s, 3H), 4.40 (s, 1H), 6.93-7.67 (m, 11H) ppm. ^{13}C NMR (100 MHz, DMSO-d_6) δ 28.17, 29.62, 36.70, 58.99, 81.25, 119.56, 127.39, 127.56, 127.56, 127.78, 128.02, 128.44, 129.37, 129.40, 129.59, 129.67, 138.72, 139.29, 140.47, 150.48, 158.20, 161.00, 161.27 ppm.

*7-Amino-5-(4-formylphenyl)-1,3-dimethyl-2,4-dioxo-1,3,4,5-tetrahydro-2H-pyrano[2,3-d]pyrimidine-6-carbonitrile (**7t**).* White solid; mp: 240–242 °C; IR (KBr) (ν_{max}, cm^{-1}) 3380, 3316, 3192, 3074, 2984, 2195, 1708, 1685, 1638, 1487, 1386, 1226, 1185, 1040, 1115, 847, 751, 698, 571. ^{1}H NMR (400 MHz, DMSO-d_6) δ 3.116 (s, 3H), 3.386 (s, 3H), 4.403 (s, 1H), 7.341-7.672 (m,6H), 9.146, (s, 1H) ppm. ^{13}C NMR (100 MHz, DMSO-d_6) δ 28.25, 29.63, 36.70, 58.99, 81.25, 128.03, 128.44, 129.37, 129.67, 130.79, 131.81, 140.47, 150.49, 158.20, 161.01, 161.28 ppm.

4. Conclusions

In this work, we have presented for the first time SiO_2@Glu/Si(OEt)$_2$(CH$_2$)$_3$N = Mo[Mo_5O_{18}] as a green and recyclable SiO_2-based nanocatalyst. The efficiency of this catalyst was evaluated in the synthesis of pyrano[2,3-*d*] pyrimidinone derivatives. This new catalytic system showed the advantages of environmentally friendly character, easy separation, non-toxicity, mild reaction conditions, short reaction times and good reusability.

Acknowledgements

The authors would like to thank the Research Council of Yasouj University for their generous support of this research work.

5. References

1. K. Zheng, C. Shen, J. Qiao, J. Tong, J. Jin, P. Zhang, *Catalysts* **2018**, *8*, 443–454. **DOI:**10.3390/catal8100443
2. D. J. Cole-Hamilton, *Science* **2003**, *299*, 1702–1706. **DOI:**10.1126/science.1081881
3. S. X. Fei, B. Han, L. Li, P. Mei, T. Zhu, M. Yang, H. Chen, *Int. J. Hydrogen Energy* **2017**, *42,* 25942–25950. **DOI:**10.1016/j.ijhydene.2017.08.204
4. C. Dai, Y. Li, C. Ning, W. Zhang, X. Wang, C. Zhang, *Appl. Catal. A Gen.* **2017**, *545*, 97–103. **DOI:**10.1016/j.apcata.2017.07.032
5. W. Shi, J. Yu, Z. Jiang, Q. Shao, W. Su, *Beilstein J. Org. Chem.* **2017**, *13*, 1661–1668. **DOI:**10.3762/bjoc.13.160
6. M. Celebi, M. Yurderi, A. Bulut, M. Kaya, M. Zahmakiran, *Appl. Catal. B Environ.* **2016**, *180*, 53–64. **DOI:**10.1016/j.apcatb.2015.06.020
7. T. Hattori, A. Tsubone, Y. Sawama, Y. Monguchi, H. Sajiki, *Catalysts* **2015**, *5*, 18–25. **DOI:**10.3390/catal5010018
8. S. Zhang, Y. R. Lee, H. J. Jeon, W. S. Ahn, Y. M. Chung, *Mater. Lett.* **2018**, *215*, 211–213. **DOI:**10.1016/j.matlet.2017.12.106
9. B. Karami, M. Kiani, S. J. Hosseini, M. Bahrami, *New J. Chem.* **2015**, *39*, 8576–8581. **DOI:**10.1039/C5NJ01302J
10. J. E. Gholtash, M. Farahi, B. Karami, M. Abdollahi, *Acta Chim. Slov.* **2020**, *67*, 866–875. **DOI:**10.17344/acsi.2020.5825
11. Y. Guo, J. Tang, Z. Wang, Y.-M. Kang, Y. Bando, Y. Yamauchi, *Nano Eng.* **2018**, *47*, 494–502. **DOI:**10.1016/j.nanoen.2018.03.012
12. P. R. Monich, F. V. Berti, L. M. Porto, B. Henriques, A. P. N. de Oliveira, M. C. Fredel, J. C. Souza, *Mater. Sci. Eng. C Mater. Biol. Appl.* **2017**, *79*, 354–362. **DOI:**10.1016/j.msec.2017.05.031
13. D. W. Lee, B. R. Yoo, *J. Ind. Eng. Chem.* **2016**, *38*, 1–12. **DOI:**10.1016/j.jiec.2016.04.016
14. R. S. Dubey, Y. Rajesh, M. A. More, *Mater. Today: Proc.* **2015**, *2*, 3575–3579. **DOI:**10.1016/j.matpr.2015.07.098
15. X. Jiang, X. Tang, L. Tang, B. Zhang, H. Mao, *Ceram. Int.* **2019**, *45*, 7673–7680. **DOI:**10.1016/j.ceramint.2019.01.067
16. L. Zare Fekri, A. R. Darya-Laal, *Polycycl. Arom. Comp.* **2020**, *40*, 1539–1556. **DOI:**10.1080/10406638.2018.1559207
17. C. Sanchez, B. Julián, P. Belleville, M. Popall, *J. Mater. Chem.* 2015, *15*, 3559–3592. **DOI:**10.1039/b509097k
18. H. S. Barud, R. M. N. Assunção, M. A. U. Martines, J. Dexpert-Ghys, R. F. C. Marques, Y. Messaddeq, S. J. L. Ribeiro, *J. Sol-Gel Sci. Technol.* **2008**, *46*, 363–367. **DOI:**10.1007/s10971-007-1669-9
19. F. Xue, Y. Dong, P. Hu, Y. Deng, Y. Wei, *RSC Adv.* **2015**, *5*, 73684–73691. **DOI:**10.1039/C5RA11798D
20. A. Zarnegaryan, M. Moghadam, S. Tangestaninejad, V. Mirkhani, I. Mohammadpoor-Baltork, *Polyhedron* **2016**, *115*, 61–66. **DOI:**10.1016/j.poly.2016.02.003
21. Z. Shi, X. Gu, J. Peng, X. Yu, E. Wang, *Eur. J. Inorg. Chem.* **2006**, *3*, 385–388. **DOI:**10.1002/ejic.200500662
22. S. Kargar, D. Elhamifar, A. Zarnegaryan, *J. Phys. Chem. Solids* **2020**, *146*, 109601–109612. **DOI:**10.1016/j.jpcs.2020.109601
23. M. Neysi, A. Zarnegaryan, D. Elhamifar, *New J. Chem.* **2019**, *43*, 12283–12291. **DOI:**10.1039/C9NJ01160A
24. N. Veronovski, M. Sfiligoj-Smole, J. L. Viota, *Text. Res. J.* **2010**, *80*, 55–62. **DOI:**10.1177/0040517509104012
25. U. M. Garusinghe, S. Varanasi, G. Garnier, W. Batchelor, *Cellulose* **2017**, *24*, 2511–2521. **DOI:**10.1007/s10570-017-1265-2
26. U. J. Kim, S. Kimura, M. Wada, *Carbohydr. Polym.* **2019**, *222*, 114975–114980. **DOI:**10.1016/j.carbpol.2019.114975
27. N. Esfandiary, A. Nakisa, K. Azizi, J. Azarnia, I. Radfar, A. Heydari, *Appl. Organomet. Chem.* **2017** *31*, 3641–3649. **DOI:**10.1002/aoc.3641
28. D. Azarifar, R. Nejat-Yami, F. Sameri, Z. Akrami, *Lett. Org. Chem.* **2012**, *9*, 435–439. **DOI:**10.2174/157017812801322435

29. a) G. Brahmachari, B. Banerjee, *ACS Sustain. Chem. Eng.* **2014**, *2*, 2802–2812. **DOI:**10.1021/sc400312n.
b) R. M. Mohareb, R. A. Ibrahim, E. S. Alwan, *Acta Chim. Slov*. **2021**, *68*, 51–64. **DOI:**10.17344/acsi.2020.6090
30. A. Khazaei, A. Ranjbaran, F. Abbasi, M. Khazaei, A. R. Moosavi-Zare, *RSC Adv.* **2015***, 5*, 13643–13647. **DOI:**10.1039/C4RA16664G
31. M. Nogueras, J. Cobo, M. L. Quijano, M. Melguizo, A. Sánchez, M. Melgarejo, *Nucleosides Nucleotides Nucleic Acids* **1994**, *13*, 447–457. **DOI:**10.1002/jlac.198919890241
32. E. M. Grivsky, S. Lee, C. W. Sigel, D. S. Duch, C. A. Nichol, *J. Med. Chem.* **1980**, *23*, 327–329. **DOI:**10.1021/jm00177a025
33. J. Davoll, J. Clarke, E. F. Elslager, *J. Med. Chem*. **1972**, *15*, 837–839. **DOI:**10.1021/jm00278a009
34. M. Bararjanian, S. Balalaie, B. Movassag, A. M. Amani, *J. Iran. Chem. Soc.* **2009**, *6*, 436–442. **DOI:**10.1007/BF03245854
35. F. Khosravian, B. Karami, M. Farahi, *New J. Chem.* **2017**, *41*, 11584–11590. **DOI:**10.1039/C7NJ02390A
36. M. Farahi, B. Karami, R. Keshavarz, F. Khosravian, *RSC Adv.* **2017**, *7*, 46644–46650. **DOI:**10.1039/C7RA08253C
37. S. Akrami, B. Karami, M. Farahi, *RSC Adv.* **2017**, *7,* 34315–34320. **DOI:**10.1039/C7RA06240K
38. B. Karami, M. Farahi, S. Akrami, D. Elhamifar, *New J. Chem. Chem.* **2018**, *42*, 12811–12816. **DOI:**10.1039/C8NJ02699H
39. H. M. Tanuraghaj, M. Farahi, *Monatsh. Chem.* **2019**, *150*, 1841–1847. **DOI:**10.1007/s00706-019-02471-x
40. H. M. Tanuraghaj, M. Farahi, *RSC Adv.* **2018**, *8*, 27818–27824. **DOI:**10.1039/C8RA05501G
41. a) J. E. Gholtash, M. Farahi, *RSC Adv.* **2018**, *8*, 40962–40967. **DOI:**10.1039/c8ra06886k
b) R. Keshavarz, M. Farahi, B. Karami, *Acta Chim. Slov.* **2021**, *68*, 332–340. **DOI:**10.17344/acsi.2020.6266
42. E. Mollashahi, M. Nikraftar, *J. Saudi Chem. Soc.* **2018**, *22*, 42–48. **DOI:**10.1016/j.jscs.2017.06.003
43. T. S. Jin, L. B. Liu, Y. Zhao, T. S. Li, *J. Chem. Res.* **2005**, *3*, 162–163. **DOI:**10.3184/0308234054213672
44. M. A. Zolfigol, R. Ayazi-Nasrabadi, S. Baghery, *Appl. Organomet. Chem.* **2016**, *30*, 273–281. **DOI:**10.1002/aoc.3428
45. M.M. Heravi, A. Ghods, K. Bakhtiari, F. Derikvand, *Synth. Commun.* **2010**, 40, 1927–1931. **DOI:**10.1080/00397910903174390
46. N. Sheikhan-Shamsabadi, M. Ghashang, (2017). *Main Group Met. Chem.* **2017**, 40, 19–25. **DOI:**10.1515/mgmc-2016-0034

Povzetek

Prispevek opisuje pripravo in identifikacijo SiO_2@Glu/Si$(OEt)_2(CH_2)_3N$ = Mo$[Mo_5O_{18}]$ kot novega bifunkcionalnega kislinsko-baznega katalizatorja (s kislimi in bazičimi Lewisovimi mesti). Najprej so aminopropiltrietoksisilan reagirali s heksamolibdatnimi anioni in nato obdelali z glukozo, ter tako pripravili Glu/Si$(OEt)_2(CH_2)_3N$ = Mo$[Mo_5O_{18}]$. Nano-siliko so nato modificirali s pripravljenim kompleksom glukoza/molibdat in dobili SiO_2@Glu/Si$(OEt)_2(CH_2)_3N$ = Mo$[Mo_5O_{18}]$. Razvit katalizator so okarakterizirali z FT-IR, EDX, XRD, FE-SEM in TGA analizo. Katalitsko učinkovitost novega katalizatorja so raziskali na primeru priprave derivatov pirano[2,3-*d*]pirimidina z reakcijo med različnimi aldehidi, malononitrilom in barbiturno kislino. Načrtovane produkte so pripravili v prisotnosti 0,004 g pripravljenega katalizatorja z visokim do odličnim izkoristkom.